J MATER SCI **41** (2006) 1059–1066

Study of artificial aging in AlMgSi (6061) and AlMgSiCu (6013) alloys by Positron Annihilation

T. E. M. STAAB*, R. KRAUSE-REHBERG
Martin-Luther Universität Halle-Wittenberg, Department of Physics, Friedemann-Bach-Platz 6, D-06108, Halle/Saale, Germany

U. HORNAUER†, E. ZSCHECH‡
Airbus Deutschland GmbH, Hünefeldstraße 1-5, D-28199, Bremen, Germany

Published online: 4 February 2006

We investigate the artificial aging process of the weldable Al-alloys AA-6013 (AlMgSiCu) and AA-6061 (AlMgSi) by positron annihilation spectroscopy and Vickers micro-hardness measurements. We find a correlation between a minimum of the measured positron lifetime and the maximum hardness. To explain these findings AlZn will be discussed as a well known example of positron interaction with different types of precipitations in aluminum. Additionally, we calculate positron annihilation parameters for pure Al, Si, Mg, and Mg_2Si finding support for our interpretation. For AA-6013 and AA-6061 the increase of the average positron lifetime after reaching the maximum hardness is attributed to the formation of semi-coherent precipitates. Hence, using positron annihilation it is possible to follow very sensitively the precipitation sequence even in technical aluminum alloys. Finally, we discuss which implications the aging may have on microstructural changes.

1. Introduction

Precipitation hardening of aluminum alloys was detected by chance. 1906 Wilm was investigating AlCuMg alloys of different chemical composition and found that the hardness increased significantly by storing the samples a couple of days at room temperature after solution heat treatment [1]. This effect was explained in the 1930th independently by Guinier and Preston [2, 3]. Aging at room or higher temperature leads to ordered meta-stable microstructural phases in the nanometer range. Directly after formation they are called *Guinier-Preston zones* (GPZ). They do not possess a crystalline structure and transform for longer aging times to ordered meta-stable phases, which are *coherent* (no mismatch dislocations) in the host matrix and effectively hinder dislocation movement. Hence, they significantly improve tensile strength or hardness. This means it is possible to tailor desired material properties by a certain sample treatment [4]. As for long aging times or high temperatures these meta-stable phases usually become first *semi-coherent* (mismatch dislocation in one crystallographic direction) and later *incoherent* (no fit to any crystallographic direction of the host matrix), they do not hinder the dislocation movement as effectively as before. Hence, the material will become softer again on overaging.

Technical properties of many alloys are well known and have been improved empirically in the past. But knowledge about the nano-structure and its effect on material properties is decisive to understand the underlying mechanisms [5]. Hence, nowadays the characterization of microstructure in the nano-size region should employ investigations by different methods.

It may be just a matter of taste what is called the microstructure of a solid. In classical terms this would mean a metallographic picture taken by an optical microscope—revealing structures down to a size of some microns—or a Transmission Electron Microscopy (TEM)-picture on the dislocation network or the distribution of precipitations characterized by their strain-field—in high resolution TEM (HRTEM) also by their size and shape. However,

Permanent Address: HISKP, Universität Bonn, Nußallee 14-16, D-53115, Bonn, Germany.
†*Permanent Address*: Forschungszentrum Rossendorf, P.O. Box 51 01 19, D-01314, Dresden, Germany.
‡*Permanent Address*: AMD Saxony LLC & Co. KG, Wilschdorfer Landstraße 101, D-01109, Dresden, Germany.
0022-2461
DOI: 10.1007/s10853-005-3640-x

there are also other—may be more indirect—methods to access the microstructure. We do mean here especially integral methods like classical X-ray diffraction (including small-angle scattering) but also modern EXAFS measurement employing synchrotron light sources and—last not least—positron annihilaiton spectroscopy (PAS), which has become a powerful tool in investigations of lattice defects in solid state physics. PAS is known since the 1980th to be a suitable method for characterizing changes in the precipitation structure of age-hardenable aluminum alloys (AlZn: [6, 7], AlZnMg: [7, 8], AlCu: [9], AlZnCuMg: [10], and for a recent review see [11, 12]). Positron annihilation also probes vacancies and vacancy-like defects and may thus detect vacancy binding to solute atoms.

Here, the important point is that, while being only minor sensitive to the shape of precipitations, positron annihilation is very sensitive to changes from fully coherent to semi-coherent precipitates as shown in Fig. 1, which in turn is a characteristic feature of the microstructure of Al-alloys, since it results in macroscopic changes like a hardness decrease.

Let us make one point clear: in common Al-alloys all alloying elements have a higher positron affinity than the Al-matrix. Since positron trapping is not primarily related to the shape of precipitates, the positrons will become localized inside the precipitations, since their mean distance in the alloys under inverstigation is roughly one order of magnitude smaller than the mean positron diffusion length (300 nm). Only in the overaged stage the precipitations might have coarsened so much that some of the positrons are not any more able to reach a precipitate. This would be reflected cleary in a change of the annihilation parameters recorded by positron lifetime spectroscopy, but which has not been observed here. Since we can assume that all positrons are finally localized inside the precipitates, the annihilation signal stemms exclusively from the influence of the internal microstructure of the precipitates (crystal structure and build in defects as well as chemical composition), or from the interface (see Fig. 1). Hence, positron annihilation spectroscopy is a very sensitive methods for recording changes in the microstructure of the precipitates and their interface, especially the change from totally coherent to semi-coherent like in Al-Zn.

While TEM provides a qualitative analysis of the size and shape of precipitates as well as an analysis of their chemical composition in the nanometer range [5], a combination with integral methods like small-angle X-ray scattering, or positron annihilation spectroscopy can provide additional information. Compared to other methods, the main drawback of TEM is the difficult sample preparation and the small volume fraction that can be investigated.

6XXX AlMgSi alloys have been developed for applications in the automotive industry, however they are used in railway waggons and aircraft fuselages, too. In contrast to AA-2024 (AlCuMg alloy), these alloys have less specific weight, and they are weldable. For the Airbus aircrafts A318 and A380, laser-beam welding has been introduced into serial production for skin-stringer joining in some fuselage sections. The precipitation sequence of 6XXX AlMgSi-alloys without major additions of copper is as follows [13, 14]: homogenization $\rightarrow$ GPZ $\rightarrow$ needle-like $\beta'' \rightarrow$ rodlike $\beta' \rightarrow \beta - Mg_2Si + Si$. The metastable phases β'' and β' transform after sufficient long heat treatment into the stable $\beta - Mg_2Si$ phase [14–16]. Copper influences the precipitation sequence and leads to the formation of additional phases: homogenization $\rightarrow$ GPZ $\rightarrow$ needle-like $\beta'' \rightarrow$ rodlike β' + lathlike $Q' \rightarrow Q + \beta - Mg_2Si + \Theta - Al_2Cu + Si$ [15, 16]. The distribution of the precursor metastable state (β'') of Mg_2Si precipitates in the age-hardenable 6XXX-alloys is one of the main factors that controls their mechanical properties [13, 17]. Copper additions results in a substantial increase in strength, since this is leading to smaller and finer distributed precipitates [18]. Increased copper concentrations lead to the formation of the so-called Q phase and its precursor Q'. It has been assumed to be an intermetallic $Al_4CuMg_5Si_4$-phase which has a rod-like shape [13], while more recent investigation propose $Al_5Cu_2Mg_8Si_4$ for its hexagonal structure [15].

The β''-phase is homogeneously distributed in the volume and totally coherent in the Al matrix. It has the shape of needles with spherical cross section, while the shape of

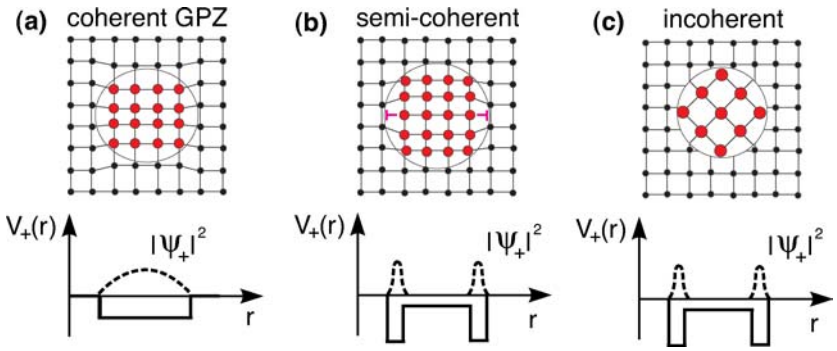

Figure 1 Localization of positron in different types of precipitations: (a) fully coherent, (b) semi-coherent and (c) incoherent. Shown are atomic positions of Al-atoms (smaller) and precipitated atoms (larger) as well as the created attractive potential for positrons (V_+) and the localization of the positron wave function (ψ_+).

the meta-stable β' phase is rod-like with ellipsoidal cross section. This phase is mostly coherent while at the ends of the rods it is incoherent to the Al-matrix—a so called semi-coherent precipitate. The shape of the $\beta - Mg_2Si$ phase is plate-like. While they have a size of some 100 nm, the depth of the plates is at least 10 nm. Its crystal structure has been determined to be the cubic CaF_2-structure with $a_0 = 0.639$ nm (see [15] and references therein). This equilibrium phase is incoherent to the Al-matrix.

The change from totally coherent to semi-coherent precipitations is important, since it influences material properties like tensile strength or hardness. However, this change is difficult to observe. Positron annihilation spectroscopy is one of the few methods which react very sensitive to these changes (see [11, 12] for a review and [19] where positron trapping to precipitates is discussed). The advantage is that PAS is non-destructive and allows statistical data on many precipitations. By lifetime spectroscopy it is in principle possible to determine the relative fraction of coherent and semi-coherent precipitations.

Even though TEM investigations are a suitable tool to monitor changes in the density and distribution of precipitations in Al-alloys, in this study accompanying TEM investigations were not necessary, since there exist a variety of studies on these and similar alloys [15–17, 20–22]. Additionally, they would not give much new information which could be correlated directly to the positron annihilation results. The reasons are as follows: Firstly, for the ageing conditions considered here the density of precipitations is so high (or their mean distance is so small) that anyway all positrons are trapped to precipitations. Secondly, the precipitations in AlMgSi alloy change during the ageing treatment applied from GPZ or clusters to fully coherent β'' at peak-age and to semi-coherent β' on over-aging, which is visible in TEM, but anyway well known from the literature. Thirdly, structural vacancies inside and local changes around precipitations are visible by PAS but not in the TEM. Hence, even here a correllation is difficult. Lastly, TEM is a local method probing only a very limited volume of about some μm^3 while positron annihilation as an integral method probes a volume of about a cm^3.

The aim of this article is to show that it is possible to follow the changes in hardness during aging AlMgSiCu-alloys at ambient temperatures (190°C) by combined positron lifetime and Doppler broadening measurements. Our interpretation of the data will be supported by a comparison to the well known system AlZn and by calculations of positron annihilation parameters.

2. Experimentals

The investigated samples where prepared form the technical aluminum alloys AA-6013 and AA-6061 provided by ALCOA. The chemical composition of the investigated AA-6013 and AA-6061 alloys are given in Table I in wt% and in at%. This means that the AA-6061 alloy is mainly quarterny (Al, Mg, Si, Cu) with a slight excess of Si and low Cu content, while the AA-6013 alloy is also mainly quarterny possessing more excess Si and a high Cu content. Stoichiometric AlMgSi alloys would have an at% relation between Mg and Si of 2:1, due to the equilibrium phase Mg_2Si.

The samples were solution heat treated at 570°C and subsequently quenched in water. After solution heat treatment and quenching for the positron measurement the source-sample sandwich with two identical samples was prepared and artificially aged at 190°C for the given time and then measured at room temperature. Without any changes of the source-sample sandwich the following heat treatment and PAS measurements have been performed. That ensures that even small changes in the average positron lifetime are recorded correctly.

As radioactive source we used ^{22}Na as positron emitter. The obtained spectra have been analyzed after source and background subtraction assuming both one and two component spectra. The decision how many components could be resolved has been made according to a comparison of the variance of the fit. We recorded 5.4×10^6 counts per spectrum after background subtraction—enough for a secure decomposition. For details on the experimental measurement and the data analysis see [19, 23–25].

To reduce the scattering due to inhomogeneities in the samples the Vickers hardness measurement has been performed as an average value of 10 points taken.

3. Positron interaction with precipitations

The quantitative description of positron trapping in precipitations has been discussed thoroughly in recent articles [11, 19]. Here, we will just briefly explain how positrons interact with precipitations.

3.1. Positron trapping into precipitations

The interaction of positrons is possible as well with coherent as with semi- or in-coherent precipitations (for the first comprehensive review on this subject see [10] or for more recent ones [11, 12]). For fully coherent precipitations the following conditions for positron trapping have to be fulfilled: (i) the positron affinity of the precipitate

TABLE I Specification for the Al-alloys AA-6013 and AA-6061

Alloy content	Mg	Si	Cu	Fe	Mn	Al
AA-6061 [wt%]	1.06	0.65	0.28	0.37	0.04	Balance
AA-6013 [wt%]	1.0	0.7	0.9	0.3	0.3	Balance
AA-6061 [at%]	1.2	0.62	0.12	0.18	0.02	Balance
AA-6013 [at%]	1.1	0.67	0.38	0.14	0.15	Balance

has to be larger than that of the surrounding matrix [26], and (ii) the totally coherent precipitates have to be larger than a critical size of some nm to allow positron capture [27]. Alloying elements like Mg, Si, Cu, Li, Zn, ... typically used in the case of Aluminum alloys fulfill the first condition [26]. The second condition is usually fulfilled shortly after quenching the sample and storage at room temperature. For semi- or in-coherent precipitates positrons may be trapped by the misfit dislocations at the interface between matrix and precipitate either directly or after having been trapped to the coherent part of a semi-coherent precipitation (see Fig. 1).

3.2. Positron annihilation at precipitations

The positron lifetime and the Doppler broadening of the annihilation radiation (DBAR) will differ significantly, whether positrons will be trapped to fully coherent precipitation on the one hand and to semi- or in-coherent precipitation on the other hand. Hence, PAS provides valuable information on the kind of a precipitate: coherent, semi-coherent, in-coherent, or coherent but containing vacancies (cf. [10, 19]). Employing the DBAR technique one can obtain additional information on the chemical environment of the positron trapping site [28, 29], i.e. the nearest neighbor atoms around a vacancy or inside the precipitation.

3.3. AlZn as an example

The results on Al-Zn containing 15 at% Zn, prepared from 4N starting material, presented in the following serve as an example for a suitable interpretation of the positron annihilation data obtained here in the case of AA-6XXX alloys.

The results for Al-Zn are just been given to show how the change from coherent to semi-coherent precipitates may be monitored by positron annihilation. This is independent of the actual shape of the precipitates (spherical, plate- or needle-like).

After solution heat treatment (450°C for 3 hours) of the AlZn-alloy, subsequent quenching in water at room temperature, and pre-aging for one hour all precipitations in the matrix are totally coherent. This is reflected in a high hardness and in the fact that the positron lifetime spectra, taken at room temperature, are single-component ($\tau_1 = 155$ps) while both lifetime and S-parameter, as given in Table II [10, 30] are in between the corresponding bulk values for Zn and Al, respectively (see [6] for the experimental details). This can only be explained by trapping sites which do not contain open volume defects like vacancies. Totally coherent precipitations with a larger positron affinity than the Al-matrix fulfill this condition. Since the precipitations are small in size and fine distributed, all positrons will reach them during their diffusive motion [8, 30].

During isothermal aging at 100°C, and hence growth of the precipitates, an increasing number of the initially fully coherent particles grow in size and become semi-coherent. This is reflected in the detection of a second lifetime component ($\tau_2 = (240 \pm 10)$ps) starting from an aging time of about 1×10^4 s, while the shorter one ($\tau_1 = (155 \pm 3)$ps) does not change. While the second lifetime is significantly longer than that detected in Al-bulk, its value of about 240ps is close to that detected for monovacancies in pure aluminum (cf. Table II [10, 30]). For even longer aging times the relative number of positrons η_2 annihilating with this new kind of trap increases, reflected also in an increasing intensity I_2 of the second lifetime component (cf. Fig. 3). The measured defect specific positron lifetime of about 240 ps can be attributed to trapping into misfit dislocations at the matrix-precipitate interface. If the positron is first trapped in the shallow potential of the precipitation itself and if there are existing misfit dislocations, then the positron certainly leaves this precursor trap and becomes localized in the deep vacancy-like trap (misfit dislocations) leading to 240 ps. Hence, positrons react very sensitive to the transition coherent → semi-coherent precipitation [6]. In principle, the trapped fraction of positrons η_2 corresponding to the longer lifetime component τ_2 should reflect the relative fraction of semi-coherent to totally coherent precipitations.

This interpretation goes conform with results on the Guinier-radius determined by small-angle X-ray scattering showing a splitting (see Fig. 2) and, hence, indicating the growth of precipitations ellipsoidal in shape. The formation of these semi-coherent precipitates is accompanied by a decrease of the hardness (see Fig. 2).

4. Results on 6013 and 6061 Al-alloys

In this section we present experimental result on the technical AA-6013 and AA-6061 alloys and theoretical calculations of positron annihilation parameters in pure Al, Si, and Mg as well as in Mg_2Si precipitations with and without vacancies. For the investigated alloys the state after solution heat treatment, quenching and two weeks

TABLE II Positron lifetimes τ and relative S-parameters S/S_{Al} for pure Al, pure Zn, the AlZn-alloy, and defect specific value for monovacancies (V_{Al}, V_{Zn}) according to Dlubek *et al.* [10, 30]. The positron is supposed to be de-localized over the entire coherent precipitation, while for semi-coherent ones it should be localized at the misfit dislocations.

Trap	Bulk Al	V_{Al}	Bulk Zn	V_{Zn}	Coherent GP-zone Al-Zn	Semi-coherent GP-zone Al-Zn
τ [ps]	160 ± 3	240 ± 5	152 ± 3	220 ± 10	155 ± 3	240 ± 10
S/S_{Al}	1.000(5)	1.040(5)	0.890(5)	0.966(5)	0.911(2)	0.997(5)

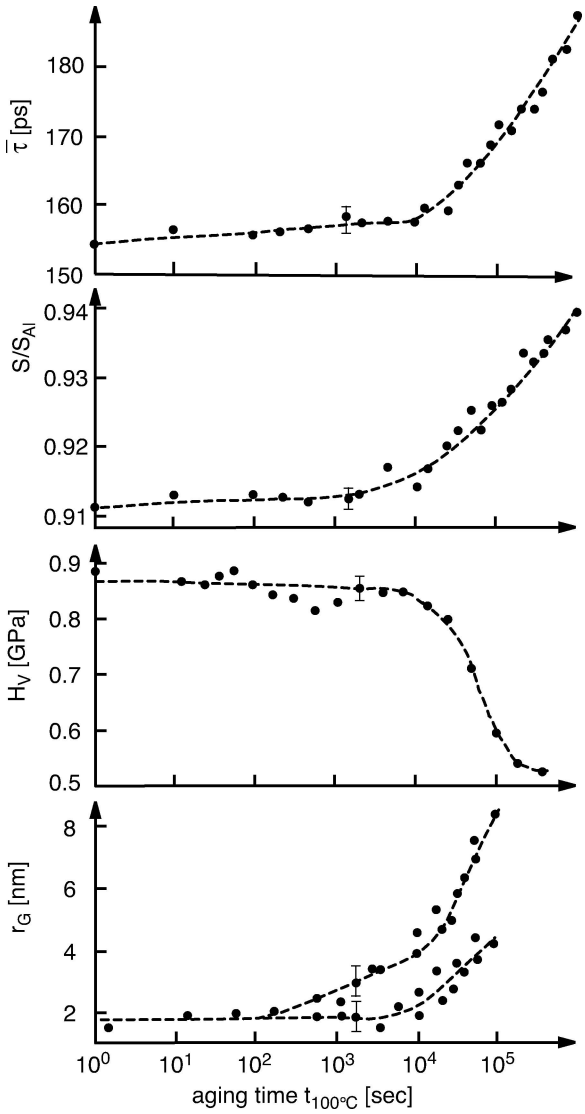

Figure 2 Relative S-parameter S/S_{Al}, average lifetime $\bar{\tau}$, and Vickers micro-hardness H_V, as well as radii of Guinier-Preston zones r_G determined by small-angle X-ray scattering for isothermal aging of Al-Zn(15) alloy at 100°C after quenching from 450°C to room temperature according to [6].

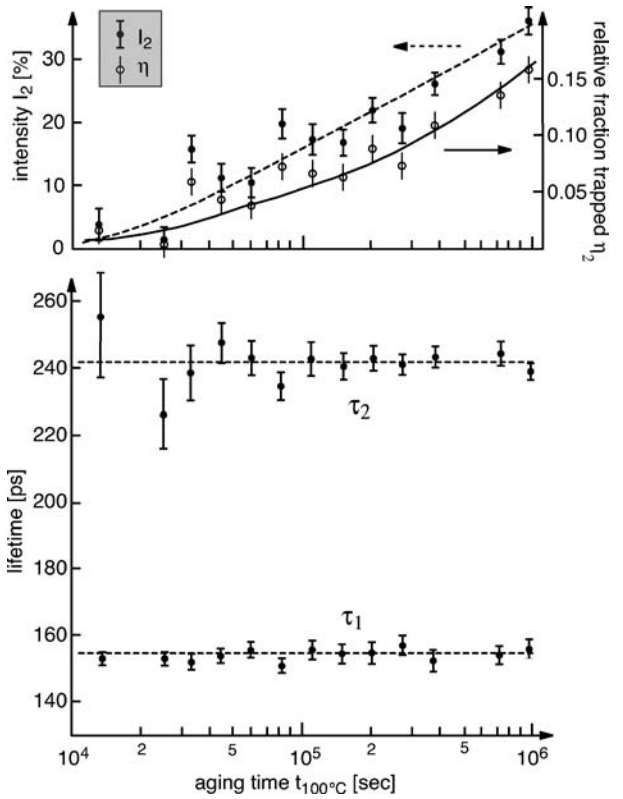

Figure 3 Decomposition of the lifetime spectra for isothermal aging of Al-Zn(15) alloy at 100°C starting from aging times $\geq 1 \times 10^4$ s according to [6]. η_2 is the relative fraction of trapped positrons corresponding to the longer lifetime τ_2.

aging at room temperature is called T4, while the state after aging at 190°C for four hours is called T6. Both sample treatments are leading to precipitates which are responsible for positron trapping. But for the final material properties in these Al-Mg-Si-Cu alloys the thermal history is decisive [15].

4.1. Calculation of positron lifetimes in Mg_2Si precipitations

The lattice structure of the β-phase (Mg_2Si) has been determined to be cubic (CaF_2 structure) with a lattice constant of $a_0 = 0.639$ nm [14, 16]. This has been used as an input for the calculations.

The calculations employ the superimposed atom method for the calculation of the positron lifetime [31, 32]. The results are given in Table III. While these calculation re-produce the positron bulk lifetime for most transition metals very well within a few, the calculations for Al are known to overestimate the bulk lifetime by at least 8 ps. The same may be the case for Mg bulk which has the same inner shell electron structure as Al.

From Table III one can see some difference for the positron lifetime corresponding to vacancies on different sublattices in Mg_2Si. The defect specific positron lifetime for vacancies on the Magnesium sublattice is longer than for vacancies on the silicon sublattice in Mg_2Si.

The positron lifetime (the inverse of the annihilation rate) is known to scale with the electron density. Since

TABLE III Positron lifetimes in bulk and defects (vacancies and divacancies) by experiment and calculations. The upper rows show the results of the calculations, while the lower rows give some experimental data (for Al see [10, 19], for Si see [33], and for Mg see [34])

	τ_b [ps]	τ_v [ps]	τ_v [ps]	τ_{divac} [ps]
		Theory		
Al	166	240	–	–
Mg	235	299	–	–
Si	221	270	–	310
Mg_2Si	238	Si: 262	Mg: 280	307
		Experiment		
Al	158 ± 3	240 ± 5	–	–
Mg	225 ± 5	–	–	–
Si	218 ± 2	275 ± 5	–	310 ± 6

the volume density of the meta-stable precipitates can be assumed to be nearly the same as that of the stable Mg_2Si crystal, this can be expected also for the electron density and, hence, the calculated positron lifetimes are expected to deviate not significantly.

4.2. Positron lifetime and Doppler broadening experiments

In both alloys the average positron lifetime measured directly after solution heat treatment and quenching is significantly above the Al-bulk lifetime: (215 ± 1) ps and (212 ± 1) ps for AA-6013 and AA-6061, respectively. For both alloys the lifetime analysis shows single component spectra—indicating only one kind of positron trap within the sensitivity limits of the method [24]. In both cases the measured positron lifetime is in between the bulk lifetime for Al and that for bulk Mg_2Si (see Table III and Fig. 5). This is indicating, as in the case of Al-Zn (cf. Section 3.3), that trapping occurs to totally coherent precipitations. The slight difference in the average lifetime between the two alloys may reflect the different copper content.

For AA-6013 the average lifetime is slightly decreasing during the hardness increase up to 120 min at 190°C (see Fig. 4). The positron lifetime spectrum remains single-component and the average lifetime is dropping from 206 down to 203 ps. At this point the hardness has reached its maximum value of 145 H_V, while the average positron lifetime reached its minimum value of 203 ps (see Fig. 4). For even longer aging times the average positron lifetime is increasing again, while the hardness tends to decrease (see Fig. 4). A two component analysis of the lifetime spectra reveals that for longer aging times than 660 min a second defect-related positron lifetime in the range 260–330ps appears with increasing intensity, while the shorter lifetime τ_1 remains constant ((203 ± 8)ps) within the error margins of the decomposition.

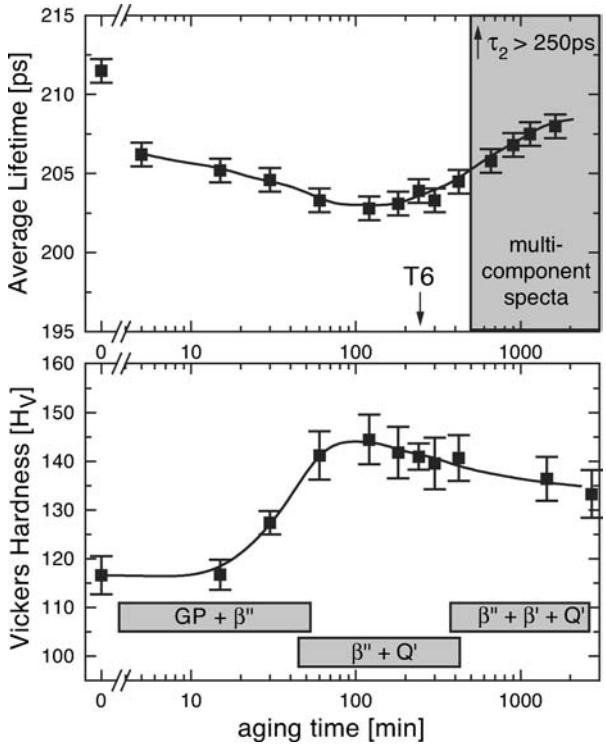

Figure 4 Average positron lifetime and hardness measurement for the alloys AA-6013 during heat treatment at 190°C. The precipitation sequence as known from the literature is indicated. The average lifetime decreases until 120 min aging time for AA-6013 while the hardness increases. Thereafter the average lifetime increases again and the spectra become two-component (indicated in the figure).

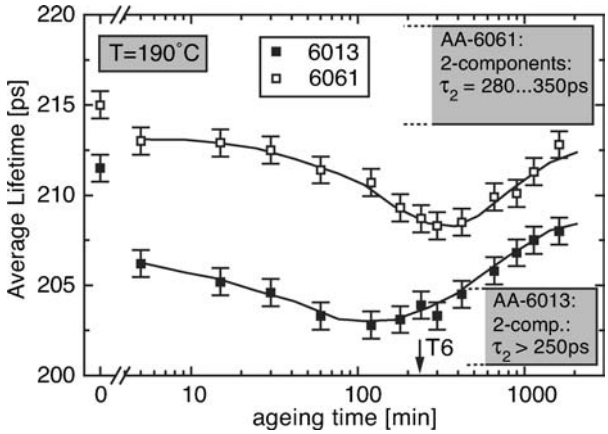

Figure 5 PAS measurement for the alloys AA-6061 and AA-6013 during heat treatment at 190°C. The average lifetime decreases until 120 min and 300 min aging time for AA-6013 and AA-6061, respectively. Thereafter the average lifetime increases again and the spectra become two-component. In the case of AA-6061 the average lifetime has its minimum toward longer aging times.

For the second investigated alloy AA-6061 a similar decrease of the average positron lifetime is observed — just a bit shifted towards longer aging times. The average positron lifetime falls from 213 ps down to 208 ps at 300 min, i.e. the minimum is reached later compared to AA-6013 (see Fig. 5). As for the more copper rich alloy AA-6013 but for shorter aging times two component spectra with a second lifetime in the range of 280 . . . 350 ps are detected with increasing intensity, while the shorter lifetime component stays approximately constant at (208 ± 5)ps. Unfortunately, the intensity is so small so that the longer lifetime component cannot be reliably resolved (for problems of the lifetime analysis see [24]), while for both alloys the value of the average lifetime is found inbetween the value for Al-bulk and Mg_2Si-bulk. This can be interpreted just as in the example discussed for Al-Zn in section 3.3. During the first hours of aging only coherent precipitates trap positrons (the average lifetime is found inbetween the value for Al-bulk and Mg_2Si-bulk). As soon as enough of the precipitations become semi-coherent or incoherent a second positron lifetime with increasing intensity appears while the first lifetime is not changed, meaning that an increasing fraction of positrons is trapped in semi-coherent precipitates (see Fig. 5 and compare $\bar{\tau}$ in Fig. 2). The positron lifetime value obtained from the decomposition of the spectra

(280–330 ps) is reasonable, since for positron annihilation in semi-coherent precipitations one would expect a specific positron lifetime as for dislocations which is usually very close to that for trapping into monovacancies—about 280ps for Mg_2Si according to Table III.

It may be interesting to note that the difference in the average lifetime between the alloys 6013 and 6061 decreases from the nearly constant value of 8 ps to 4 ps just during the hardness increase (see Fig. 5). The lifetime difference between AA-6013 and AA-6061 could be an indication of the enhanced formation of the copper-rich so-called Q'-phase in the case of AA-6013. The lattice structure of this phase is suggested to be similar to that of Mg_2Si. But different author propose different chemical compositions: $Al_4CuMg_5Si_4$ [13] and $Al_5Cu_2Mg_8Si_5$ [14].

Additional DBAR experiments have been performed at the same time. They show a similar trend for the S-parameter with aging time as the average positron lifetime does. For the W-parameter (sensitive to core-electron annihilation) the trend shows that over the considered aging time the W-parameter is always higher for AA-6013 compared to AA-6061. It has been noted earlier that positron annihilation in the vicinity of copper atoms increases significantly in the very momentum range where the W-parameter is taken. The data are omitted here due to their poor statistics.

5. Conclusions

The results presented here show that it is possible to follow changes in the precipitation structure during ambient temperature aging (T6) of the technically important Al-alloys 6XXX. At an aging time when the maximum hardness is detected, the average positron lifetime reaches a minimum while the spectra become two-component due to new formed open volume defects associated with an increasing fraction of the precipitates. This is indicating the formation of semi- or incoherent additional phases. The longer positron lifetime typical for semi- or in-coherent precipitates is also reflected in the increasing average positron lifetime.

Hence, we have shown that by means of positron annihilation it is possible to follow the changes in the precipitation structure, i.e. the transition from coherent to semi-coherent, for the aluminum alloys AA-6013 and AA-6061. Significant changes in the lifetime spectra have been correlated with changes in the hardness of the samples.

For the future one could imagine aging at slightly higher or lower temperatures than 190°C and over-aging the material significantly to produces the incoherent equilibrium phases. Detailed analysis of the core-annihilation of positrons via DBAR measurements are expected to give more concise information on the chemical surrounding of the annihilation sites inside the precipitations or at their interface towards the aluminum matrix.

Considering not previously characterized Al-alloys produced e.g. from high purity elements, it would be highly desirable to combine positron annihilation measurements with structural investigations by transmission electron microscopy to correlate the obtained PAS-data in a unique way with changes in the microstructure like the transition from coherent to semi-coherent precipitates.

Acknowledgment

We would like to thank Dr. Christiane Zamponi and Prof. K. Maier (both University Bonn) for comments on the manuscript.

References

1. A. WILM, *Metallurgie*, **8** (1911) 255.
2. A. GUINIER, *Ann.Phys.*, **12** (1938) 161 .
3. G. D. PRESTON, *Phil. Mag.*, **26** (1938) 855.
4. J. E. HATCH, *Aluminum—Properties and Physical Metallurgy*. American Society for Metals, Ohio, 1984.
5. D. B. WILLIAMS, Modern microstructural analysis of aluminum alloys, edited by T. H. Sanders and E. A. Starke, *Proc. 4th Int. Conf. on Aluminum Alloys*, Atlanta, 1994, Vol. 3, pp. 50–66.
6. R. KRAUSE, G. DLUBEK and G. WENDROCK, *Cryst. Res. Technol.* **20**(11) (1985) 1495.
7. G. DLUBEK, O. BRÜMMER and R. KRAUSE, *Crys. Res. Technol.* **20** (1985) 275.
8. G. DLUBEK, R. KRAUSE, O. BRÜMMER and F. PLAZAOLA, *J. Mater. Sci.* **21** (1986) 853.
9. U. H. GLÄSER, G. DLUBEK and R. KRAUSE, *Mater. Sci. Forum* **105–110** (1992) 1025.
10. G. DLUBEK, *Mater. Sci. Forum* **13–14** (1987) 15.
11. A. DUPASQUIER, P. FOLEGATI, N. DE DIEGO and A. SOMOZA, *J. Phys.: Condens. Matter* **10** (1998) 10409.
12. A. DUPASQUIER, G. KÖGEL and A. SOMOZA, *Acta Materialia*, **52** (2004) 4707.
13. B. THANABOONSOMBUT and T. H. SANDERS, A review of the physical metallurgy of 6013, edited by T. H. Sanders and E. A. Starke, *The 4th International Conference on Aluminum Alloys* (Atlanta, 1994), pp. 197–201.
14. L. SAGALOWICZ, G. HUG, B. BECHET, P. SAINFORT and G. LAPASSET, A study of the structural precipitation in the Al-Mg-Si-Cu system, edited by T. H. Sanders and E. A. Starke, *The 4th International Conference on Aluminum Alloys*, (Atlanta, 1994), pp. 636–643.
15. W. F. MIAU and D. E. LAUGHLIN, *Metallurgical and Materials Transactions A* **31A** (2000) 361.
16. D. J. CHAKRABARTI, YINGGUO PENG and DAVID E. LAUGHLIN, *Mater. Sci. Forum*. **396–402** (2002) 857.
17. W. F. MIAU and D. E. LAUGLIN, *Scripta Materialia* **40**(7) (1999) 873.
18. D. W. PASHLEY, J. W. PHODES and A. SENDOREK, *J. Inst. Met.* **94** (1966) 41.
19. T. E. M. STAAB, E. ZSCHECH and R. KRAUSE-REHBERG, *J. Mater. Sci.* **35** (2000) 4667.
20. G. A. EDWARDS, K. STILLER, G. L. DUNLOP and M. J. COUPER, *Acta mater.* **46**(11) (1998) 3893.
21. M. MURAYAMA and K. HONO, *Acta mater.* **47**(5) (1999) 1537.
22. A. K. GUPTA, D. J. LLOYD and S. A. COURT, *Mater. Sci. Eng.* **A316** (2001) 11.
23. R. KRAUSE-REHBERG and H. S. LEIPNER, *Positron Annihilation in Semiconductors* (Springer Verlag, Berlin, 1999).
24. B. SOMIESKI, T. E. M. STAAB and R. KRAUSE-REHBERG, *Nucl. Instr. Meth. Phys. Res.* **A381** (1996) 128.
25. T. E. M. STAAB, B. SOMIESKI and R. KRAUSE-REHBERG, *Nucl. Instr. Meth. Phys. Res.* **A381** (1996) 141.
26. M. J. PUSKA, P. LANKI and R. M. NIEMINEN, *J. Phys.: Condens. Matter* **1** (1989) 6081.

27. G. BISCHOF, V. GRÖGER, G. KREXNER and R. M. NIEMINEN, *J. Phys.: Condens. Matter* **8** (1996) 7523.
28. P. ASOKA-KUMAR, M. ALATALO, V. J. GHOSH, A. C. KRUSEMAN, B. NIELSEN and K. G. LYNN, *Phys. Rev. Lett.* **77**(10) (1997) 2097.
29. M. ALATALO, B. BARBIELLINI, M. HAKALA, H. KAUPPINEN, T. KORHONEN, M.J. PUSKA, K. SAARINEN, P. HAUTOJÄRVI and R. M. NIEMINEN, *Phys. Rev.* **B54**(4) (1996) 2397.
30. G. DLUBEK, O. BRÜMMER and R. KRAUSE, Classification of positron traps in age-hardenable Al-alloys, edited by P. C. Jain, R. M. Singru and K. P. Gopinathan, *Proccedings of the 7th Int. Conf. on Positron Annihilation, New Dehli, India*, Singapore, 1985. World Scientific, p. 883.
31. M. J. PUSKA and R. M. NIEMINEN, *J. Phys. F: Metal Phys.* **13** (1983) 333.
32. M. J. PUSKA and R. M. NIEMINEN, *Rev. Mod. Phys.* **66**(3) (1994) 841.
33. A. POLITY, F. BÖRNER, S. HUTH, S. EICHLER and R. KRAUSE-REHBERG, *Phys. Rev. B* **58**(16) (1998) 10363.
34. P. HAUTOJÄRVI, J. JOHANSSON, A. VEHANEN, J. YLI-KAUPPILA, J. HILLAIRET and P. TSANETAKIS, *Appl. Phys.*, **A27** (1982) 49.

Received 22 July 2003
and accepted 25 May 2005